Relative Localization for Moving Robot Formations

Martin W. Freeman
dept. of Aeronautics & Astronautics
Stanford University
Stanford, USA
emmerich@stanford.edu

***Abstract*—Accurate localization of agents in applications involving moving robot formations is core to not only the safety of mobile robots in unknown environments, but also the integrity of the accompanying formation control strategies. Instruments such as ultra-wideband radios are progressively gaining popularity as ranging sensors to support relative localization in multi-robot systems, introducing a nonlinear measurement model as a consequence. An Unscented Kalman Filter (UKF) is implemented to estimate the state of such a multi-robot system over the commonly implemented Extended Kalman Filter (EKF) alternative given the preferable naturality of the UKF's sigma point propagation over the EKF's linearization approach. The accuracy, stability, convergence time and computational complexity of the constructed UKF will be explored and compared to the EKF.**

I. Introduction

Cooperative state estimation is an important feature of any network of mobile robots that have unforgiving requirements on localization accuracy. Planetary exploration is one particular application that often introduces such requirements via the commonly harsh environments mobile robots (i.e a rover) are subjected to. Safe exploration of a GPS-denied environment without an *a priori* map is very often a core goal, considering the potential mission failure given an unrecoverable misstep taken due to poor localization. Networks of multiple robots such as JPL's Dasher [1] project travel in a moving formation to perform subsurface mapping, necessitating robust formation control and further highlighting the need for accurate relative localization. One proposed tool to support these types of systems is time-based ranging via ultra-wideband (UWB) radio, a popular sensor candidate for relative localization that has proven the potential to be very accurate for close-range positioning [2]. With the increasing pervasiveness of UWB-based ranging for relative localization in applications where agents are cooperative [7], increased interest in the analysis of state estimation methods for these range-based measurement systems should naturally follow.

Equipping each robot in a network with the ability to measure distances between one another presents a system with a nonlinear measurement model in addition to the likely nonlinear dynamics of each node in the system. While an Extended Kalman Filter (EKF) would allow us to estimate the state of the nonlinear system with a first order approximation, the suboptimal nature of it's uncertainty estimation and stability qualities encourage the consideration of other solutions. One such solution, the Unscented Kalman Filter (UKF), can describe a nonlinear system more accurately than a characterization based on the first-order Taylor expansion term, whilst enjoying a better level of accuracy and stability than the EKF given similar system complexity [3]. In the UKF, a set of gaussian-distributed sigma points are sampled and transformed through the nonlinear function, where the gaussian is then reconstructed from the transformed sigma points. This the *Unscented Transform* and it is used as an alternative to the linearization performed in the EKF. Additionally, Jacobians are evaluated precisely by the UKF, presenting a convenient derivative-free estimation formulation. One notable drawback to the UKF is a consistent slight constant-time increase in computation time over the EKF, though there have been several approaches [9] that push that computation time toward the EKF's in select instances.

In this project, the Unscented Kalman Filter algorithm will be implemented on the nonlinear system consisting of two mobile robots with unicycle dynamics and ranging sensors with error akin to current UWB ranging hardware [5]. Chosen due to it's superior properties as it relates to estimation of highly nonlinear systems, the UKF's performance when used for 2-dimensional relative localization of two adjacent robots will be explored in terms of accuracy, stability, convergence time and computational complexity.

II. System Formulation

A. Overview

A multi-robot network consisting of 2 nodes will have each node described by unicycle dynamics and have each node travelling along a trajectory precomputed according to the desired formation between the nodes. The sensor information available for each node consists of the node's own odometry measurement as well as a unique range measurement distance to the other node (i.e both robots have UWB transmitters and receivers). Errors in sensor measurement and process noise follow a gaussian distribution and the robots have a constant line of sight between one another.

B. Robot Dynamics

Instead of dealing with the unnecessary complexity of lower-level dynamics of a differential drive system, we make use of the much simpler unicycle model below for each robot in the formation

$$\mathcal{U} = \begin{bmatrix} \dot{x} \\ \dot{y} \\ \dot{\phi} \end{bmatrix} = \begin{bmatrix} V\cos\phi \\ V\sin\phi \\ \omega \end{bmatrix} \quad (1)$$

Where V, ω are inputs

C. System Dynamics

As we are considering relative localization and have no notion of global coordinates, we perform our state estimation in terms of transformation matrices T_{21} and T_{12} between the two robots. The subscript *21* indicates a transformation *from* the coordinate frame of robot 2 *to* the coordinate frame of robot 1. That is, x_{21}, y_{21},θ_{21} describe the relative position and angle of robot 2 to robot 1 (Figure 1).

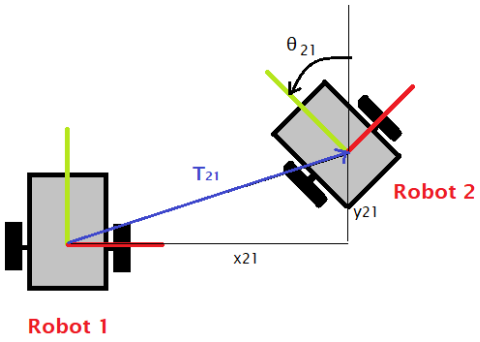

Figure 1: Depiction of coordinate transform T_{21}

The system state can thus be represented as the stacked transformation matrices T_{21} and T_{12}

$$\mathbf{x} = \begin{bmatrix} T_{21} \\ T_{12} \end{bmatrix} = \begin{bmatrix} x_{21} \\ y_{21} \\ \theta_{21} \\ x_{12} \\ y_{12} \\ \theta_{12} \end{bmatrix}$$

In accordance with the unicycle model, we describe our system inputs in terms of each robot's linear and angular velocities $v_1, v_2, \omega_1, \omega_2$,

$$\mathbf{u} = \begin{bmatrix} v_1 \\ \omega_1 \\ v_2 \\ \omega_2 \end{bmatrix}$$

The transformation matrices have the motion models below,

$$\dot{T_{21}} = \begin{bmatrix} v_2 cos(\theta_{21}) \\ v_2 sin(\theta_{21}) \\ \omega_2 \end{bmatrix} + \begin{bmatrix} y_{21}\omega_1 - v_1 \\ -x_{21}\omega_1 \\ \omega_1 \end{bmatrix}$$

$$\dot{T_{12}} = \begin{bmatrix} v_1 cos(\theta_{12}) \\ v_1 sin(\theta_{12}) \\ \omega_1 \end{bmatrix} + \begin{bmatrix} y_{12}\omega_2 - v_2 \\ -x_{12}\omega_2 \\ -\omega_2 \end{bmatrix}$$

Where the first term in each transformation reflects the dynamics of the unicycle model. That is, the first term of $\dot{T_{21}}$ represents the effect of robot 2's vehicle dynamics on the transform T_{21}. While the second term represents the effect of v_1 and ω_1 for robot 1 on T_{21}.
A discrete-time approximation to the continuous-time dynamics is performed to generate the state transition function. First order Euler discretization is used to define the state transition, a comparatively simple method over alternatives such as higher-order Runge-Kutta methods. Euler discretization approximates the derivative operator as

$$\dot{\mathbf{x}} = \begin{bmatrix} \dot{T_{21}} \\ T_{12} \end{bmatrix} \approx \frac{\dot{x}[k+1] - \dot{x}[k]}{dt}$$

Where *dt* is a sample time chosen small enough to minimize appreciable approximation error. We also note that this is a non-linear gaussian process, and as such we will have zero-mean gaussian process noise $\mathbf{w}$ with covariance Q ($\mathbf{w} \sim \mathcal{N}(0, Q)$). In this model, we consider it to be more reasonable for the process noise to reflect in the direct system inputs $v_1, v_2, \omega_1, \omega_2$ alone rather than adding a general process noise to the state evolution. Denoting This yields the overall state evolution model with non-additive noise,

$$\mathbf{x}[k+1] = f(\mathbf{x}[k], \mathbf{w}[k], \mathbf{u}[k]) = \mathbf{x}[k] + \dot{\mathbf{x}}[k]dt$$

where $\dot{\mathbf{x}}[k]$ is

$$\dot{\mathbf{x}} = \begin{bmatrix} (v_2 + w_3)cos(\theta_{21}) \\ (v_2 + w_3)sin(\theta_{21}) \\ (\omega_2 + w_4) \\ (v_1 + w_1)cos(\theta_{12}) \\ (v_1 + w_1)sin(\theta_{12}) \\ (\omega_1 + w_2) \end{bmatrix} + \begin{bmatrix} y_{21}(\omega_1 + w_2) - (v_1 + w_1) \\ -x_{21}(\omega_1 + w_2) \\ (\omega_1 + w_2) \\ y_{12}(\omega_2 + w_4) - (v_2 + w_3) \\ -x_{12}(\omega_2 + w_4) \\ -(\omega_2 + w_4) \end{bmatrix}$$

evaluated at timestep *k* with $(\mathbf{x}[k], \mathbf{w}[k], \mathbf{u}[k])$.

D. Sensor Measurement Model

The measurement model consists of two independent ranging measurements between the two robots and four odometry measurements corresponding to our simplified unicycle model inputs, a vector which we will denote as $\mathbf{y}_o$. As with the motion model, in all of our outputs we observe an additive zero mean gaussian measurement noise $\boldsymbol{\nu}$ of covariance R ($\boldsymbol{\nu} \sim \mathcal{N}(0, R)$). Both odometry and ranging measurements are

drawn from sensors, and thus must realistically be expected to carry some error. We assume a uniform covariance for the measurement error across both types of outputs and formulate the measurement model as

$$\mathbf{y}_o[k] = g(\mathbf{x}[k], \mathbf{u}[k]) + \boldsymbol{\nu}[k]$$

$$\mathbf{y}_o = \begin{bmatrix} d_{21} \\ d_{12} \\ v_1 \\ \omega_1 \\ v_2 \\ \omega_2 \end{bmatrix} + \boldsymbol{\nu} = \begin{bmatrix} \sqrt{x_{21}^2 + y_{21}^2} \\ \sqrt{x_{12}^2 + y_{12}^2} \\ v_1 \\ \omega_1 \\ v_2 \\ \omega_2 \end{bmatrix} + \begin{bmatrix} \nu_1 \\ \nu_2 \\ \nu_3 \\ \nu_4 \\ \nu_5 \\ \nu_6 \end{bmatrix}$$

E. Observability

Guarantees on observability for the moving formation system must be met before the UKF can be implemented. The work performed here [6] contains an observability analysis for multi-robot systems equipped with proprioceptive and exteroceptive sensors (odometry and UWB ranging information, respectively). While the paper concludes that a system using relative bearing measurements provides the best observability, obtaining relative bearing measurements is typically harder than obtaining a range estimate and often requires visual analysis. Despite being suboptimally observable, observability analysis of the relative distance measurement system is performed and [6] contends that the measured linear velocity of both robots in our systems must be non-zero for the state to be fully observable. That is, $v_1 \neq 0$, $v_2 \neq 0$

III. Method

A. Overview

Our analysis seeks to explore performance in terms of accuracy, stability, convergence time of the UKF applied to the system described in section II. Two robots with identical dynamics and differing initial estimates of the transform between each other's coordinate frames are subjected to a predetermined control scheme, resulting in the change of both coordinate frames over time. The stacked transform matrices describe the state of the system, and evolve stochastically over time as influenced by the process noise. An online estimate of this state is deduced by applying the prediction and correction steps of the UKF. Rather than linearize our state estimate around the mean as in an EKF-based solution, we transform a set of weighted sigma points through the non-linear state evolution model and reconstruct a gaussian estimate of the new state from the resultant output. A correction to the state and state covariance estimation is then calculated based on the current measurement. These two steps are repeated with each estimation iteration.

B. Prediction Step

Given initial estimates of the mean, $\mu_{0|0}$, and state covariance, $\Sigma_{0|0}$, for $\mathbf{x} \in \mathbf{R}^n$, where $n = 6$, we perform the *unscented transform* below to obtain $2n + 1$ sigma points $\mathcal{X}$ in $\mathbf{R}^n$ and $2n + 1$ weights $\mathcal{W}$ in $\mathbf{R}$

$$(\boldsymbol{\mu}_{t-1|t-1}, \boldsymbol{\Sigma}_{t-1|t-1}) \xrightarrow{\text{UT}} \{\mathcal{X}_{t-1|t-1}, \mathcal{W}_{t-1}\}$$

$$\mathcal{X}_{t-1|t-1} = \{\boldsymbol{\mu}_{t-1|t-1}, (\boldsymbol{\mu}_{t-1|t-1} + \sqrt{(n+\lambda)\boldsymbol{\Sigma}_{t-1|t-1}})_i, (\boldsymbol{\mu}_{t-1|t-1} - \sqrt{(n+\lambda)\boldsymbol{\Sigma}_{t-1|t-1}})_i\}$$

$$\text{for ith column} = 1, 2, ..., n$$

$$\mathcal{W} = \{\frac{\lambda}{n+\lambda}, (\frac{1}{2(\lambda+n)})_i \mid i = 1, 2, ..., 2n\}$$

We then perform the sigma point prediction by propagating our sigma points and inputs u_{t-1} through the state evolution function of the system and obtain the updated predictions $\bar{\mathcal{X}}^*_{t|t-1}$ in sigma point form,

$$\bar{\mathcal{X}}^*_{t|t-1} = f(\mathcal{X}_{t-1|t-1}, \mathbf{u}_{t-1})$$

We then need to perform the inverse unscented transform to reconstruct the gaussian for the state prediction,

$$(\bar{\mathcal{X}}^*_{t|t-1}, \mathcal{W}) \xrightarrow{\text{UT}^{-1}} (\boldsymbol{\mu}_{t|t-1}, \boldsymbol{\Sigma}_{t|t-1})$$

$$\boldsymbol{\mu}_{t|t-1} = \sum_{i=0}^{2n} w_m^{[i]} \overline{\mathcal{X}}_t^{*[i]}$$

$$\boldsymbol{\Sigma}_{t|t-1} = \sum_{i=0}^{2n} w_c^{[i]} \left(\overline{\mathcal{X}}_t^{*[i]} - \bar{\mu}_t\right)\left(\overline{\mathcal{X}}_t^{*[i]} - \bar{\mu}_t\right)^T + Q_t$$

Where Q_t is a term that encodes the estimate of the non-additive process noise covariance and λ is a parameter that incorporates knowledge about the distribution of the state in the generation of the sigma points ($\lambda = 2$ is optimal for a gaussian distribution).

C. Correction Step

Similar to the above, we will now perform correction of the state estimate based on the current measurement and our propagated estimates of the mean $\mu_{t|t-1}$ and state covariance $\Sigma_{t|t-1}$ by again considering the sigma-point representations of our propagated state $\bar{\mathcal{X}}^*_{t|t-1}$. First, we propagate $\bar{\mathcal{X}}^*_{t|t-1}$ and u_{t-1} through our measurement model to obtain the sigma-point measurements, $y^{[i]}_{t|t-1}$ (i.e what we would measure if these points were our true state) and construct an expected measurement $\mathcal{Y}_{t|t-1}$,

$$y^{[i]}_{t|t-1} = g(\overline{\mathcal{X}}^*_{t|t-1}, \mathbf{u}_{t-1})$$

$$\mathcal{Y}_{t|t-1} = \sum_{i=0}^{2n} w^{[i]} y^{[i]}_{t|t-1}$$

We can now construct an empirical covariance of the measurement $\Sigma^Y_{t|t-1}$ and an empirical state-measurement cross-covariance $\Sigma^{XY}_{t|t-1}$ as,

$$\Sigma^{Y}_{t|t-1} = \sum_{i=0}^{2n} w^{[i]}(y^{[i]}_{t|t-1} - \mathcal{Y}_{t|t-1})(y^{[i]}_{t|t-1} - \mathcal{Y}_{t|t-1})^T + R_t$$

$$\Sigma^{XY}_{t|t-1} = \sum_{i=0}^{2n} w^{[i]}(\mathcal{X}^{*[i]}_{t|t-1} - \mu_{t|t-1})(y^{[i]}_{t|t-1} - \mathcal{Y}_{t|t-1})^T$$

Where R_t is the covariance that encodes our knowledge about the measurement model's noise. We can now finalize the correction step by utilizing our predicted state and state covariances as well as the empirical covariances in the gaussian estimation equations to update our estimates $\mu_{t|t}$ and $\Sigma_{t|t}$

$$\mu_{t|t} = \mu_{t|t-1} + \Sigma^{XY}_{t|t-1}(\Sigma^{Y}_{t|t-1})^{-1}(y_t - \mathcal{Y}_{t|t-1})$$
$$\Sigma_{t|t} = \Sigma_{t|t-1} - \Sigma^{XY}_{t|t-1}(\Sigma^{Y}_{t|t-1})^{-1}(\Sigma^{XY}_{t|t-1})^T$$

Where y_t denotes the real sensor measurement at the current timestep.

IV. Results

The UKF and EKF were implemented for varying values of Q, R the initial state estimate μ_0 and the initial covariance estimate, Σ_0 for a period of $T = 12$ seconds with a sampling time of $dt = 0.05$.

A. Stability

1) Nominal Performance ($Q = dtI_4$, $R = .1I_6$, $\Sigma_0 = I_6$, $\mu_0 - x_0 \approx 0$):

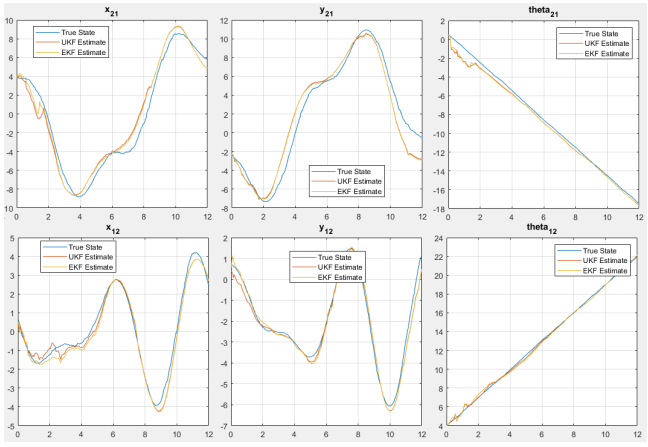

Figure 2: Nominal Performance of UKF, EKF

With nominal parameters and relatively good guesses for the initial state and covariance, both filters perform identically and do not differ in their convergence. For varying Q and R, both filters continue to perform similarly without a difference in convergence.

2) Varying Σ_0:

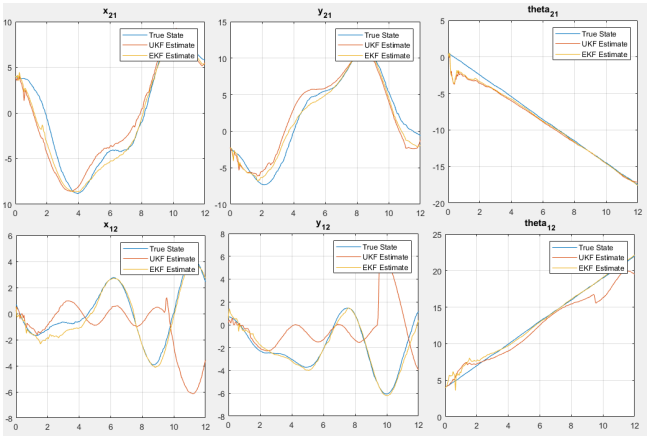

Figure 3: Poor Σ_0 estimate for UKF, EKF

As the initial estimate for state covariance is varied in a direction generally further from the true state covariance, the UKF was much more likely to exhibit divergent behavior, suggesting that stability for the UKF has a moderate sensitivity to Σ_0.

3) Varying μ_0:

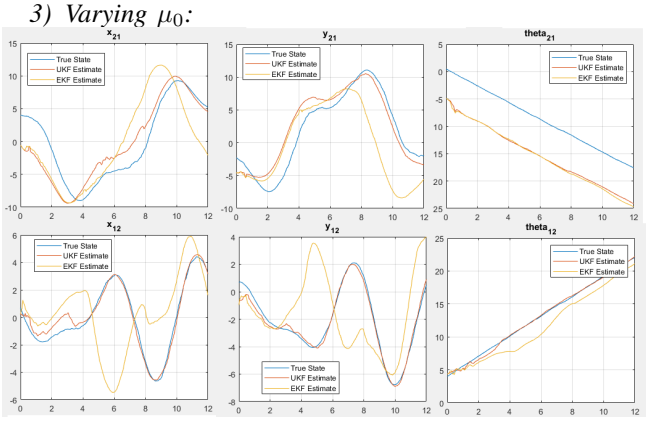

Figure 4: Poor μ_0 estimate for UKF, EKF

As the initial estimate for the state is varied to be further from the true initial state, the UKF was much less likely to diverge.

B. Time analysis

For all of the analysis trials where there was no difference in convergence between the UKF and EKF, the time to perform online estimation over the entire time interval ($T = 12s$) was calculated. The average UKF loop was found to be $80.0ms$ while the average EKF loop was found to be $73.1ms$, denoting a minor speed advantage of around 9% for the EKF.

C. Accuracy

Given an initial estimate for the state covariance Σ_0 closer to the true state covariance, and under the other nominal conditions stated above, the sum of the norm of the error residuals

for each filter differed by less than 1% on average. Overall analysis trials where there was no difference in convergence between the UKF and EKF but nominal parameters were varied, the sum of the norm of the error residuals remained below 5%, though the EKF typically had the lower value.

V. Discussion

A natural followup to the implementation of the UKF is to explore how it compares to the EKF under the same circumstances. As our 2-robot moving formation system is nonlinear but not *highly* nonlinear, we could expect the EKF to yield performance comparable to the UKF, though similar experiments [8] have determined the UKF to have greater localization accuracy and consistency. In this analysis, the UKF and EKF appear to share the same stability behavior under mild, nominal conditions. Variations in the initial estimate of state covariance Σ_0 further from the true value appear to trigger the UKF to diverge while the EKF remains convergent. [10] contends that this is often due to a lack of numerical stability in the UKF, wherein the square root covariance computation within the filter quickly loses precision in the estimate. When the initial state covariance is strong, but the initial state of the system, μ_0, varies further from the true value, the UKF appears to maintain convergence when the EKF diverges. One likely suggestion for this behavior is the very reason we chose to examine the UKF in the first place, that is, the EKF's approximation errors are magnified when the taylor expansion is used to linearize the dynamics around a highly inaccurate estimate of the state, leading swiftly to divergence. Thus, for this system in particular, the UKF provides much greater stability if our state estimates ever vary largely from the true state but we have a reasonable estimation of the state covariance.

In terms of accuracy, both filters performed too similarly to gauge an appreciable difference under mild conditions. The EKF tended to have slightly lower residuals, even given strong initialization, which is contrary to the general agreement that the UKF is more accurate. I would contend that while the system is non-linear, it not highly non-linear and thus the UKF provides no significant advantage in it's approach to dealing with the non-linearities under mild conditions.

Under mild conditions, the online estimation using the EKF was around 9% faster than the UKF, which agrees with the expectation that the EKF is typically less computationally complex.

VI. Conclusion

While the UKF can provide advantages in specific situations such as poor state initialization and highly non-linear dynamics, it performs too similarly to the EKF under reasonable conditions and provides little to no advantage in accuracy when dealing with a linear or nearly linear system. Additionally, if the initialization of the initial state covariance is very poor, the UKF may be much less stable than the EKF due to numerical error accumulation in it's square rooting of the covariance during computation. Lastly, the EKF generally performed around 10% faster for the this system, making it a more desirable choice for real-time applications it performs similarly when put up against the UKF under mild conditions.

References

[1] Nunes, Daniel C., et al. "Shifting the Paradigm of Coping with Nyx on the Moon—a Ground-Penetrating Radar Case." LPI Contributions 2106 (2018).

[2] Soganci, Hamza, Sinan Gezici, and H. Vincent Poor. "Accurate positioning in ultra-wideband systems." IEEE Wireless Communications 18.2 (2011): 19-27.

[3] Wan, Eric A., and Rudolph Van Der Merwe. "The Unscented Kalman Filter for nonlinear estimation." Proceedings of the IEEE 2000 Adaptive Systems for Signal Processing, Communications, and Control Symposium (Cat. No. 00EX373). Ieee, 2000.

[4] Ghommam, Jawhar, et al. "Formation path following control of unicycle-type mobile robots." Robotics and Autonomous Systems 58.5 (2010): 727-736.

[5] "Channel effects on communications range and time stamp accuracy in D1000 based systems" https://www.decawave.com/wp-content/uploads/2018/10/APS006_Part-1-Channel-Effects-on-Range-Accuracy_v1.03.pdf, 2020, accessed: 2020-05-05

[6] Martinelli, Agostino, and Roland Siegwart. "Observability analysis for mobile robot localization." 2005 IEEE/RSJ International Conference on Intelligent Robots and Systems. IEEE, 2005.

[7] Guo, Kexin, Xiuxian Li, and Lihua Xie. "Ultra-wideband and odometry-based cooperative relative localization with application to multi-UAV formation control." IEEE transactions on cybernetics (2019).

[8] Giannitrapani, Antonio, et al. "Comparison of EKF and UKF for spacecraft localization via angle measurements." IEEE Transactions on aerospace and electronic systems 47.1 (2011): 75-84.

[9] Huang, Guoquan P., Anastasios I. Mourikis, and Stergios I. Roumeliotis. "A quadratic-complexity observability-constrained Unscented Kalman Filter for SLAM." IEEE Transactions on Robotics 29.5 (2013): 1226-1243.

[10] Van Der Merwe, Rudolph, and Eric A. Wan. "The square-root unscented Kalman filter for state and parameter-estimation." 2001 IEEE international conference on acoustics, speech, and signal processing. Proceedings (Cat. No. 01CH37221). Vol. 6. IEEE, 2001.

[11] MATLAB Code Repository: https://github.com/emmerich-martin/aa273finalproject